

Searching for a light Fermiophobic Higgs Boson at the Tevatron

Andrew G. Akeroyd^a, Marco A. Díaz^b

*a: Korea Institute for Advanced Study, 207-43 Cheongryangri-dong,
Dongdaemun-gu, Seoul 130-772, Republic of Korea*

*b: Departamento de Física, Universidad Católica de Chile,
Avenida Vicuña Mackenna 4860, Santiago, Chile*

Abstract

We propose new production mechanisms for light fermiophobic Higgs bosons (h_f) with suppressed couplings to vector bosons (V) at the Fermilab Tevatron. These mechanisms (e.g. $qq' \rightarrow H^\pm h_f$) are complementary to the conventional process $qq' \rightarrow Vh_f$, which suffers from a strong suppression of $1/\tan^2 \beta$ in realistic models with a h_f . The new mechanisms extend the coverage at the Tevatron Run II to the larger $\tan \beta$ region, and offer the possibility of observing new event topologies with up to 4 photons.

1 Introduction

The study of extensions of the Standard Model (SM) which include more than one Higgs doublet [1] has received much attention in last 20 years. The SM predicts one neutral Higgs scalar (ϕ^0) with branching ratios (BRs) which are functions of m_{ϕ^0} . It is predicted to decay dominantly via $\phi^0 \rightarrow b\bar{b}$ for $m_{\phi^0} \leq 130$ GeV, and $\phi^0 \rightarrow VV^{(*)}$ (where $V = W^\pm, Z$) for $m_{\phi^0} \geq 130$ GeV. The minimal extension of the SM contains an additional $SU(2) \times U(1)$ Higgs doublet, the ‘‘Two Higgs Doublet Model’’ (2HDM), and the resulting particle spectrum consists of 2 charged Higgs bosons H^+, H^- and 3 neutral members h^0, H^0 and A^0 . Assuming that each fermion type (up,down) couples to only one Higgs doublet [2], which eliminates tree-level Higgs mediated flavour changing neutral currents, leads to 4 distinct versions of the 2HDM [3]. Due to the increased parameter content of the 2HDM the BRs of the neutral Higgs bosons may be significantly different to those of ϕ^0 [1],[4]. In recent years LEP2 has carried out searches [5] for such Higgs bosons with enhanced BRs to lighter fermions and bosons (e.g. $c\bar{c}, \tau^+\tau^-, gg$). The phenomena known as ‘‘fermiophobia’’ [6] which signifies very suppressed or zero coupling to the fermions, may arise in a particular version of the 2HDM called type I [7]. Such a fermiophobic Higgs (h_f)[8, 9, 10, 11, 12, 13, 14] would decay dominantly to two bosons, either $h_f \rightarrow \gamma\gamma$ (for $m_{h_f} \leq 90$ GeV) or $h_f \rightarrow VV^{(*)}$ for ($m_{h_f} \geq 90$ GeV) [10, 11]. This would give a very clear experimental signature, and observation of such a particle would strongly constrain the possible choices of the underlying Higgs sector.

Fermiophobic Higgs bosons have been searched for actively at LEP and the Tevatron. All four collaborations at LEP (OPAL[15], DELPHI[16], ALEPH[17], L3[18]) utilized the channel $e^+e^- \rightarrow h_f Z, h_f \rightarrow \gamma\gamma$ and obtained lower bounds of the order $m_{h_f} \geq 100$ GeV. L3 [19] is the only collaboration yet to consider $h_f \rightarrow WW^*$ decays. OPAL [15] and DELPHI [16] also searched in the channel $e^+e^- \rightarrow H_F A^0, H_F \rightarrow \gamma\gamma$. In run I at the Tevatron the mechanism $qq' \rightarrow V^* \rightarrow h_f V, h_f \rightarrow \gamma\gamma$ was used, with the dominant contribution coming from $V = W^\pm$. The limits on m_{h_f} from the D0 and CDF collaborations are respectively 78.5 GeV [20] and 82 GeV [21] at 95% *c.l.* Run II will extend the coverage of m_{h_f} beyond that of LEP.

However, all these mass limits assume that the $h_f VV$ coupling is of the same strength as the SM coupling $\phi^0 VV$, which in general would not be the case for a h_f in a realistic model e.g. the 2HDM (type I) or the Higgs triplet model of [22], [23]. Therefore one could imagine the scenario of a very light h_f ($m_{h_f} \ll 100$ GeV) which has eluded the current searches at LEP and the Tevatron Run I due to suppression in the coupling $h_f VV$. Such a h_f could also escape detection in the Tevatron Run II. In this paper we propose new production mechanisms at the Tevatron Run II which are effective even when the coupling $h_f VV$ is very suppressed.

Our work is organized as follows. Section 2 gives an introduction to the phenomenology of fermiophobic Higgs bosons while Section 3 presents the new production mechanisms. Section 4 contains our numerical results with conclusions in section 5.

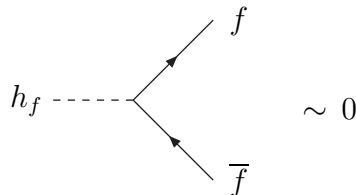
2 Models with Fermiophobia

A fermiophobic Higgs boson (h_f) may arise in a 2HDM in which one $SU(2) \times U(1)$ Higgs doublet (Φ_2) couples to all fermion types, while the other doublet (Φ_1) does not. Both doublets couple to the gauge bosons via the kinetic term in the Lagrangian. One vacuum expectation value (v_2) gives mass to all fermion types, while gauge bosons receive mass from both v_1 and v_2 . This model (usually called “Type I”) was first proposed in [7]. Due to the mixing in the CP–even neutral Higgs mass matrix (which is diagonalized by α) both CP–even eigenstates h^0 and H^0 can couple to the fermions. The fermionic couplings of the lightest CP–even Higgs h^0 take the form

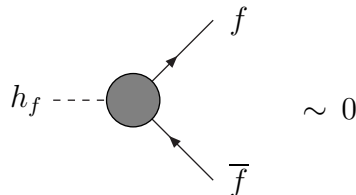
$$h^0 f \bar{f} \sim \cos \alpha / \sin \beta \quad (1)$$

where f is any fermion, and β is defined by $\tan \beta = v_2/v_1$.

Small values of $\cos \alpha$ would seriously suppress the fermionic couplings, and in the limit $\cos \alpha \rightarrow 0$ the coupling $h^0 f \bar{f}$ would vanish at tree–level, giving rise to fermiophobia (sometimes called a “bosonic” or “bosophilic” Higgs):

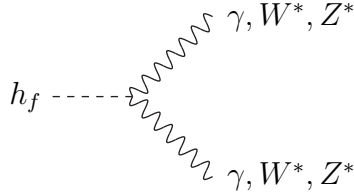


However, at the 1–loop level there will be an effective vertex $h_f f \bar{f}$ mediated by loops involving vector bosons and other Higgs particles. These loop contributions are infinite and a counterterm is necessary to renormalize it. The counterterm is fixed with an experimental input, leading to an arbitrariness in the definition of the tree level vertex, or equivalently, in the mixing angle α [11]. It is customary to define an extreme fermiophobia, where h_f remains fermiophobic to the 1-loop level/all orders with branching ratios given by [10],[11]. In general, one would expect some (small) coupling to fermions, from both tree–level diagrams and one loop diagrams.



The Higgs Triplet model (HTM) discussed in [22],[23] is another possible origin for a h_f . In such models gauge invariance forbids the tree–level coupling of some triplet Higgs bosons to fermions, and so suppressed BRs to fermions are expected without requiring specific mixing angles.

The main decay modes of a fermiophobic Higgs are:



$h_f \rightarrow \gamma\gamma$ is the dominant decay for $m_{h_f} \lesssim 95$ GeV (sometimes called a “photonic Higgs”), with a BR near 100% for $m_{h_f} \lesssim 80$ GeV, decreasing to 50% at $m_{h_f} \approx 95$ GeV and to 1% at $m_{h_f} \approx 145$ GeV. In contrast, $\text{BR}(\phi^0 \rightarrow \gamma\gamma) \approx 0.22\%$ is the largest value in the SM for the two photon decay. In this paper we shall be focusing on the possibility of a light ($m_{h_f} \leq 100$ GeV) for which the photonic decay mode always has a large BR.

$\text{BR}(h_f \rightarrow WW^*)$ supercedes $\text{BR}(h_f \rightarrow \gamma\gamma)$ when $m_{h_f} \gtrsim 95$ GeV, with a BR approaching 100% for $110 \text{ GeV} < m_{h_f} < 170 \text{ GeV}$, and stabilizing at $\sim 70\%$ for $m_{h_f} \geq 2M_Z$. The decay $h_f \rightarrow ZZ^*$ is always subdominant, but for $m_{h_f} \geq 2M_Z$ approaches 30%. Recently, L3 [19] has included these VV^* decays in their searches, and the discovery prospects of this decay mode at the Tevatron Run II have been presented in [24].

Apart from the 2HDM (Type I) and the HTM, there are other models beyond the SM which allow the possibility of a neutral Higgs boson with an enhanced BR to $\gamma\gamma$, as explained in [25]. These include h^0 of the MSSM, and h^0 of top–condensate models. We will not consider these models, which have a smaller $\text{BR}(h^0 \rightarrow \gamma\gamma)$ than the fermiophobic models, and instead focus on the 2HDM (Type I)¹. Our results can also be quite easily extrapolated to the case of the HTM.

The conventional production mechanism for a h_f at e^+e^- colliders is $e^+e^- \rightarrow Z^* \rightarrow h_f Z$, and at Hadron colliders $qq' \rightarrow V^* \rightarrow h_f V$. Note that the gluon-gluon fusion mechanism (via heavy quark loops) is not relevant for a h_f . In the 2HDM (Type I), the condition for tree–level fermiophobia ($\cos \alpha \rightarrow 0$) causes the coupling $h_f VV$ to be suppressed by a factor

$$h_f VV \sim \sin^2(\beta - \alpha) \rightarrow \cos^2 \beta \equiv 1/(1 + \tan^2 \beta) \quad (2)$$

Taking $\tan \beta \geq 3(10)$ implies a strong suppression of $\leq 0.1(\leq 0.01)$ for the coupling $h_f VV$ with respect to the coupling $\phi^0 VV$. This suppression is always possible for the lightest CP–even neutral Higgs in any of the 4 types of the 2HDM [1] and also occurs for the h_f in the HTM [23]. Therefore one can imagine the scenario of a very light h_f which has eluded the searches via the mechanisms $e^+e^-/qq' \rightarrow h_f V$. The possibility of a light h_f has been known for a long time [11] and has been emphasized in [12],[13]. LEP ruled out regions of the plane [$m_{h_f}, R \times \text{BR}(h_f \rightarrow \gamma\gamma)$], where R is defined by:

$$R = \frac{\sigma(e^+e^- \rightarrow Zh_f)}{\sigma(e^+e^- \rightarrow Z\phi^0)} \quad (3)$$

¹Another interesting possibility for a light Higgs boson with enhanced decays to $\gamma\gamma$ has been considered in [27],[28]. Here if A^0 is extremely light (≤ 0.2 GeV) then $\text{BR}(A^0 \rightarrow \gamma\gamma)$ may be large.

In a benchmark scenario of $R = 1$, and assuming $\text{BR}(h_f \rightarrow \gamma\gamma)$ given by [10], [11], each collaboration derived a limit of around $m_{h_f} \geq 100$ GeV [15],[16], [17],[18], with the combined LEP working group limit being $m_{h_f} \geq 109$ GeV [19]. From the LEP plots it is trivial to see the necessary suppression in R which would permit a light h_f of a given mass, e.g. $m_{h_f} \leq 80$ GeV (50 GeV) requires $R \leq 0.1(0.01)$, which corresponds to $\tan\beta \geq 3(10)$ in the 2HDM (Type I). Therefore sizeable regions of the $[m_{h_f}, R \times \text{BR}(h_f \rightarrow \gamma\gamma)]$ plane remain unexcluded for small R and small m_{h_f} . OPAL [15] also performed a search which is sensitive to the production mechanism $e^+e^- \rightarrow h_f A^0$. This process ($\sim \sin^2\beta$ in the fermiophobic limit) is complementary to $e^+e^- \rightarrow h_f Z$ ($\sim \cos^2\beta$). Therefore the condition $m_{h_f} + m_A \geq \sqrt{s}$ must also be satisfied in order for a light h_f to escape detection at LEP2.

With the closure of LEP, the Tevatron Run II will continue the search for h_f . Run II will use the same mechanism as Run I ($qq' \rightarrow V^* \rightarrow Vh_f$) but has the advantage of a much increased luminosity. Ref.[25] has shown that (for $R = 1$) m_{h_f} can be discovered (at 5σ) up to 114 GeV (128 GeV) with 2 fb^{-1} (30 fb^{-1}), which is an improvement over the LEP limits. Similar conclusions were reached in [26]. However, with the expected suppression in the $h_f VV$ coupling ($R < 1$), $m_{h_f} \leq 80$ GeV could still escape detection. The aim of this paper is to show that other production mechanisms are available at the Tevatron Run II, and allow discovery of a h_f even in the region where the process $qq' \rightarrow Wh_f$ is suppressed.

We will be using the most general (CP conserving) 2HDM potential [1]. This potential is parametrized by 7 independent variables, which may be taken as the four Higgs masses, two mixing angles (α, β), and a real quartic coupling (λ_5).

$$V(\Phi_1, \Phi_2) = V_{sym} + V_{soft} \quad (4)$$

where

$$V_{sym} = -\mu_1^2 \Phi_1^\dagger \Phi_1 - \mu_2^2 \Phi_2^\dagger \Phi_2 + \lambda_1 (\Phi_1^\dagger \Phi_1)^2 + \lambda_2 (\Phi_2^\dagger \Phi_2)^2 + \lambda_3 (\Phi_1^\dagger \Phi_1) (\Phi_2^\dagger \Phi_2) + \lambda_4 |\Phi_1^\dagger \Phi_2|^2 + \frac{1}{2} [\lambda_5 (\Phi_1^\dagger \Phi_2)^2 + h.c.] \quad (5)$$

and

$$V_{soft} = -\mu_{12}^2 \Phi_1^\dagger \Phi_2 + h.c. \quad (6)$$

The condition for tree-level fermiophobia corresponds to $\cos\alpha \rightarrow 0$, with α being an independent parameter. Ref. [13] considered the fermiophobic limit in the context of two 6 parameter 2HDM potentials (V_A and V_B). In Ref. [13] the angle α is not a free parameter, and the condition $\cos\alpha \rightarrow 0$ requires certain relations among the Higgs masses to be fulfilled. We shall take all the Higgs masses as free parameters and set $\cos\alpha = 0$, which guarantees tree-level fermiophobia.

3 Production Processes

In this section we introduce the production processes which may offer sizeable rates for h_f in the region where the coupling $h_f VV$ is very suppressed. These production mechanisms

make use of the cascade decays $H^\pm \rightarrow h_f W^{(*)}$ or $A^0 \rightarrow h_f Z^{(*)}$ which may have large BRs in the 2HDM (Type I) [29] and the HTM [23]. These large BRs arise since the coupling of H^\pm and A^0 to all the fermions scales as $1/\tan\beta$, and thus for moderate to large $\tan\beta$ even the 3-body decays (i.e. with V^*) can have sizeable or dominant BRs. We note that in the MSSM such decays (with h_f replaced by h^0) never attain very large BRs since H^\pm and A^0 couple to the down type fermions with strength $\tan\beta$. In addition, the decays $H^\pm \rightarrow h^0 W^{(*)}$ or $A^0 \rightarrow h^0 Z^{(*)}$ are proportional to $\cos^2(\beta - \alpha)$ which is suppressed in a large part of the MSSM parameter space, but (in contrast) is maximized in the parameter of h_f with suppressed coupling to vector bosons.

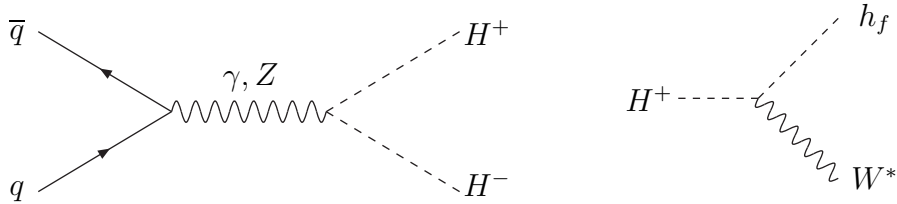
Refs.[25],[26] considered two signatures from the $qq' \rightarrow WH_F$ mechanism, i) inclusive $\gamma\gamma$ and ii) exclusive $\gamma\gamma V$. The latter gives a better signal to background ratio and we will see that the cascade decay produces the necessary vector boson for the $\gamma\gamma V$ signature.

Below we list four production processes which are complementary to the standard $qq' \rightarrow WH_F$ mechanism. They all make use of the Higgs-Higgs-Vector boson coupling (g_{HHV}) which is either proportional to $\sin\beta$ (in the fermiophobic limit) or independent of mixing angles (see Table 1). All mechanisms can offer non-negligible cross-sections in the large $\tan\beta$ region. Moreover, double H_F production can occur, resulting in distinctive $\gamma\gamma\gamma\gamma$ topologies.

| | $H^\pm AW^\mp$ | $H^\pm h_f W^\pm$ | $h_f AZ$ |
|-----------|----------------|-------------------|-------------|
| g_{HHV} | 1 | $\sin\beta$ | $\sin\beta$ |

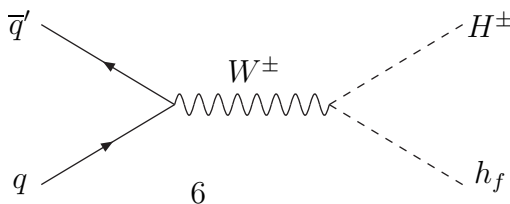
Table 1: Mixing angle dependence of the couplings $H_i H_j V$

- (i) $q\bar{q} \rightarrow \gamma^*, Z^* \rightarrow H^+ H^-$: Quark anti-quark pair annihilation produces a pair of charged Higgs bosons via an intermediate photon or Z boson in the s-channel:



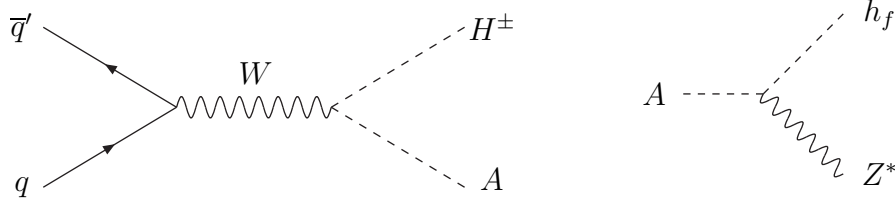
The subsequent decay $H^\pm \rightarrow h_f W^*$ may provide two W^* and two h_f , resulting in a distinctive $\gamma\gamma\gamma\gamma$ plus four fermion signal.

- (ii) $qq' \rightarrow W^* \rightarrow H^\pm h_f$: Quark anti-quark annihilation into an intermediate W boson producing a h_f in association with a charged Higgs:



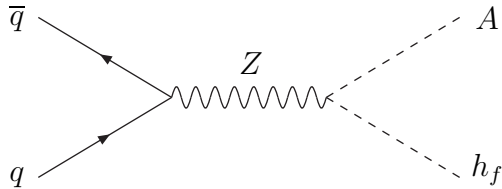
This mechanism was covered in the case of the MSSM in [30], but only for the heavier CP-even H^0 . The rate for the lighter CP-even h^0 is suppressed by $\cos^2(\beta-\alpha)$, which is small in a large region of the MSSM parameter space. The cross-sections for H^+h_f and H^-h_f are identical, and will be summed over in our numerical analysis. This process is phase space favoured over (i) and provides direct production of h_f . A vector boson (W^*) is provided by the decay $H^\pm \rightarrow W^*h_f$. In this way, double h_f production occurs with a signature of $\gamma\gamma\gamma\gamma$ plus V^* .

- (iii) $q\bar{q}' \rightarrow W^* \rightarrow H^\pm A^0$: Quark anti-quark annihilation into an intermediate W producing a charged Higgs in association with a CP-odd neutral Higgs:



This process is similar to (i) since no fermiophobic Higgs is produced directly. We sum over the rates for H^+A^0 and H^-A^0 as in (ii). The decay $H^\pm \rightarrow h_f W^*$ or $A^0 \rightarrow Z^* h_f$ provides a gauge boson V and a h_f . Again, double h_f production may occur giving rise to a final state of $\gamma\gamma\gamma\gamma V^*V^*$. This mechanism was considered in the context of the MSSM in [31].

- (iv) $q\bar{q} \rightarrow Z^* \rightarrow A^0 h_f$: Quark anti-quark pair annihilation into an intermediate Z producing a fermiophobic Higgs in association with a CP-odd neutral Higgs:



This process is similar to (ii) and gives direct production of h_f with a Z boson arising from the decay $A^0 \rightarrow h_f Z^*$. The $\gamma\gamma\gamma\gamma$ signal is also possible with this mechanism.

Mechanisms i) and iv) are the hadron collider analogies of the LEP production processes $e^+e^- \rightarrow H^+H^-$ and $e^+e^- \rightarrow A^0 h_f$, but have the advantage of the larger \sqrt{s} at the Tevatron. Mechanisms ii) and iii) are exclusive to a hadron collider. The cross-section formulae for all the processes can be found in [32],[33]. One may write a generic formula for (ii),(iii) and (iv):

$$\sigma(q\bar{q} \rightarrow H_i H_j) = \frac{G_F^2 M_Z^4}{96\pi \hat{s}} g_{HHV}^2 (v_q^2 + a_q^2) \frac{\lambda^{3/2}}{(1 - M_V^2/\hat{s})^2} \quad (7)$$

where H_i, H_j (with mass M_i, M_j) refer to any of the Higgs bosons $H^\pm, A^0, h_f, \lambda(M_i, M_j)$ is the usual two body phase space function, and \hat{s} is the centre of mass energy for the partonic collision. In eq. (7), v_q and a_q represent the vector and axial vector couplings of the incoming quarks to the vector boson mediating the process, and are given in Table 2. In the same formula, g_{HHV} is the Higgs–Higgs–Vector Boson coupling which are listed in Table 1.

| | Z | W^\pm |
|-------|---------------------------------------|----------------------------|
| v_u | $0.25 - \frac{2}{3} \sin^2 \theta_w$ | $\sqrt{2} \cos^2 \theta_w$ |
| a_u | 0.25 | $\sqrt{2}/\cos^2 \theta_w$ |
| v_d | $-0.25 - \frac{1}{3} \sin^2 \theta_w$ | $\sqrt{2} \cos^2 \theta_w$ |
| a_d | -0.25 | $\sqrt{2}/\cos^2 \theta_w$ |

Table 2: Values for v_q and a_q

4 Numerical Results

We now outline the calculation of the cross-section for the processes (i)→ (iv) under consideration. The partonic cross-sections are given by eq. (7). These must then be scaled up to a $p\bar{p}$ cross-section. In the partonic centre of mass system, the kinematic is defined as:

$$\begin{aligned}\hat{s} &= (p_q + p_{q'})^2 = (p_{H_i} + p_{H_j})^2 \\ \hat{t} &= \frac{1}{2}(M_{H_i}^2 + M_{H_j}^2) - \frac{\hat{s}}{2} + \frac{\hat{s}}{2}\kappa \cos \theta \\ \hat{u} &= \frac{1}{2}(M_{H_i}^2 + M_{H_j}^2) - \frac{\hat{s}}{2} - \frac{\hat{s}}{2}\kappa \cos \theta \\ \hat{s} + \hat{t} + \hat{u} &= M_{H_i}^2 + M_{H_j}^2\end{aligned}$$

Here $\kappa^2 = (\hat{s} - (M_{H_i} + M_{H_j})^2)(\hat{s} - (M_{H_i} - M_{H_j})^2)/\hat{s}^2$. The hadronic cross-section for the process $p\bar{p} \rightarrow qq' \rightarrow H_i H_j$ can be expressed as follows:

$$\sigma(p\bar{p} \rightarrow qq' \rightarrow H_i H_j) = \int_{(M_{H_i} + M_{H_j})^2/s}^1 d\tau \frac{d\mathcal{L}^{q\bar{q}}}{d\tau} \hat{\sigma}(\hat{s} = \tau s). \quad (8)$$

In the case of the Tevatron Run II $\sqrt{s} = 2$ TeV.

$$\frac{d\mathcal{L}^{q\bar{q}}}{d\tau} = \int_\tau^1 \frac{dx}{x} f_q(x; Q^2) f_{q'}(\tau/x; Q^2) \quad (9)$$

where $\tau = x_1 x_2$, with x_1 and x_2 being the momentum fraction carried by each incoming parton. The parton distributions f_q and $f_{q'}$ shall be taken at the typical scale $Q \approx M_{H_i}$. We shall be using the MRST2002 set from [34]. Note that QCD corrections increase the

tree-level cross-section by a factor of around 1.3 [33]. In our analysis we shall present results using the tree-level formulae only. For the BRs of the fermiophobic Higgs we also work at tree-level and set $\cos\alpha = 0$ to ensure exact fermiophobia.

The four new production mechanisms under consideration are generally expected to be ineffective for searches where the Higgs boson decays to quarks, since backgrounds will be sizeable. However, in the case of h_f we will show that they offer promising detection prospects despite the moderate cross-sections. This is because the efficiency for the $\gamma\gamma V$ channel is high ($\approx 25\%$) [25], and the decays $H^\pm \rightarrow h_f W^*$ or $A^0 \rightarrow Z^* h_f$ may have very large BRs in the 2HDM (Model I) discussed here. In much of the parameter space of interest ($\tan\beta \geq 1$ and $m_{h_f} < 100$ GeV), $\text{BR}(H^\pm \rightarrow h_f W^{(*)})$ and $\text{BR}(A^0 \rightarrow Z^{(*)} h_f)$ are close to 100%. Hence a light h_f can be produced in a cascade with almost negligible BR suppression (see [29] for a quantitative analysis of these BRs). The cascade decays provide distinctive $\gamma\gamma\gamma\gamma$ signatures from all four mechanisms. In our numerical analysis we will vary m_{h_f} with particular emphasis on $m_{h_f} < 100$ GeV. We will take $m_{H^\pm} \geq 90$ GeV (roughly the lower bound from LEP2) and M_A is constrained by $m_A + m_{h_f} \geq 200$ GeV from negative searches in the channel $e^+e^- \rightarrow h_f A^0$. For the expected 2 fb^{-1} of data from Run IIa, which might be available by 2005/2006, we assume a threshold of observability of 10 fb for the cross-sections. Larger data samples of up to 15 fb^{-1} would require even smaller values.

In Fig. 1 we plot all five mechanisms as a function of $\tan\beta$ for fixed values of the CP-odd Higgs mass $m_A = 150$ GeV, charged Higgs mass $m_{H^\pm} = 90$ GeV, and fermiophobic Higgs mass $m_{h_f} = 50$ GeV. For a fermiophobic Higgs of this mass to escape detection at LEP2 one requires $\tan\beta > 10$. The traditional mechanism $p\bar{p} \rightarrow W^\pm h_f$ dominates at low $\tan\beta$ as expected, but falls fast with increasing $\tan\beta$ due to the $\cos^2\beta$ suppression mentioned earlier. For $\tan\beta > 10$ all the new mechanisms offer larger cross-sections than the traditional one. The process $p\bar{p} \rightarrow H^\pm h_f$ is dominant for $\tan\beta \gtrsim 3$ with a cross-section growing from 30 fb for $\tan\beta = 0.5$ up to 155 fb for $\tan\beta = 50$. In the parameter space of interest ($\tan\beta \geq 10$) one finds $\text{BR}(H^\pm \rightarrow h_f W^*) \approx 100\%$ and so this mechanism essentially leads to a signature of $\gamma\gamma\gamma\gamma$ plus W^* .

The $p\bar{p} \rightarrow H^+ H^-$ mechanism has a production cross-section of 29 fb and is independent of $\tan\beta$. This cross-section becomes larger than $\sigma(p\bar{p} \rightarrow W^\pm h_f)$ at $\tan\beta \approx 7$, and leads to a signature of $\gamma\gamma\gamma\gamma$ plus $W^* W^*$. Similarly, $p\bar{p} \rightarrow H^\pm A^0$ has a cross-section $\sigma = 14$ fb (independent of $\tan\beta$) and supercedes the traditional mechanism at $\tan\beta \approx 10$. As above, h_f is produced via a cascade decay, which also provides the vector boson. Both $H^\pm \rightarrow h_f W^*$ and $A^0 \rightarrow h_f Z^*$ are effectively 100% which leads again to the $\gamma\gamma\gamma\gamma$ plus $V^* V^*$ signature. The behaviour of $\sigma(p\bar{p} \rightarrow A^0 h_f)$ with $\tan\beta$ is similar to that of $p\bar{p} \rightarrow H^\pm h_f$. It grows with $\tan\beta$ and is essentially constant for large values of that parameter. This mechanism produces a fermiophobic Higgs directly, but has a lower rate due to the constraint $m_{h_f} + m_A \geq 200$ GeV. Since $\text{BR}(A^0 \rightarrow h_f Z) \approx 100\%$ the $\gamma\gamma\gamma\gamma$ plus V^* signature also arises from this mechanism.

In Fig. 2 we plot the five mechanisms as a function of the charged Higgs mass m_{H^\pm} , for a constant value of the fermiophobic Higgs mass $m_{h_f} = 50$ GeV. We also fix $\tan\beta = 20$ which ensures that a h_f of this mass would have had too low a rate to be detected at

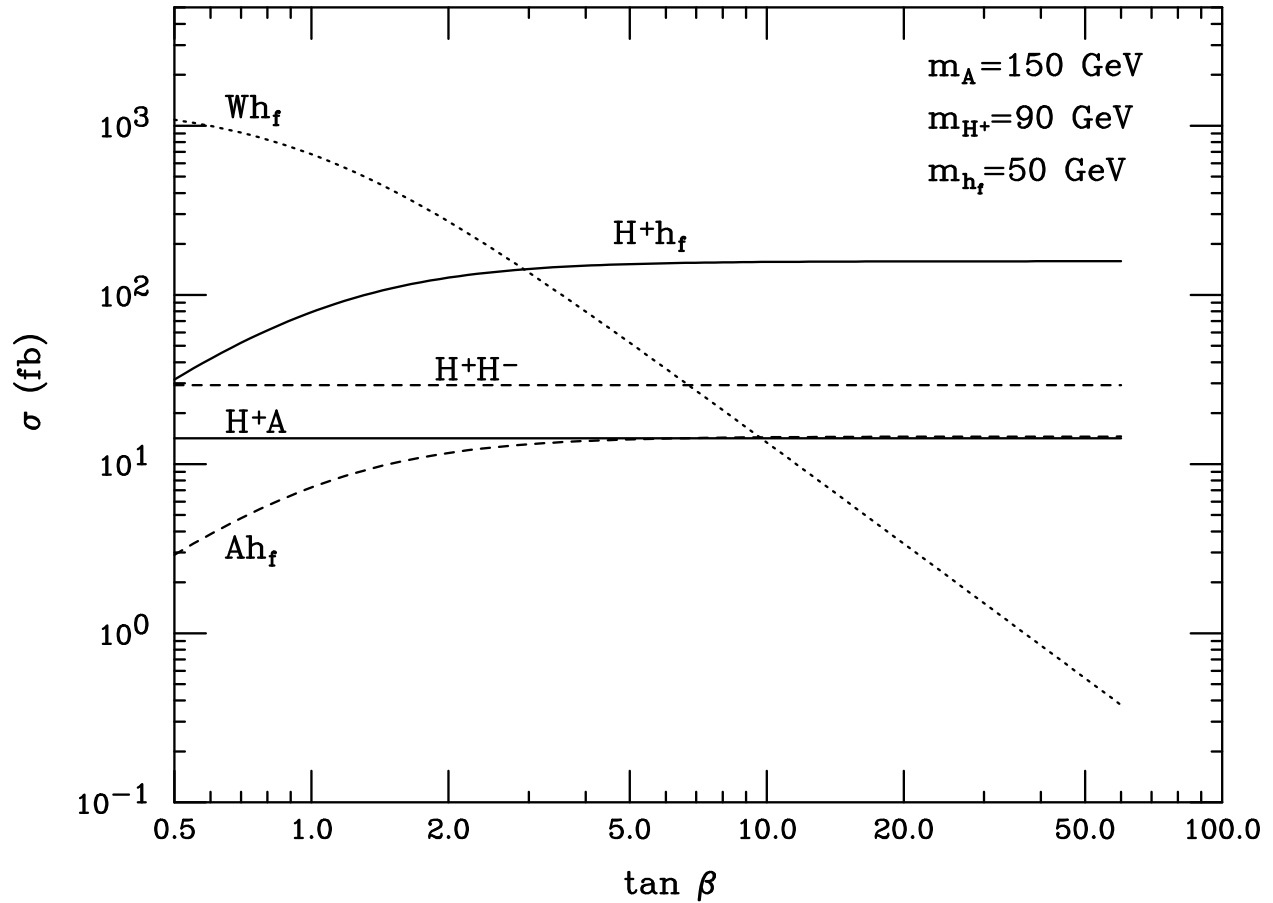


Figure 1: *Production cross-section of five different modes leading to a fermiophobic Higgs boson as a function of $\tan \beta$, for fixed values of the charged, the CP-odd, and the fermiophobic Higgs masses.*

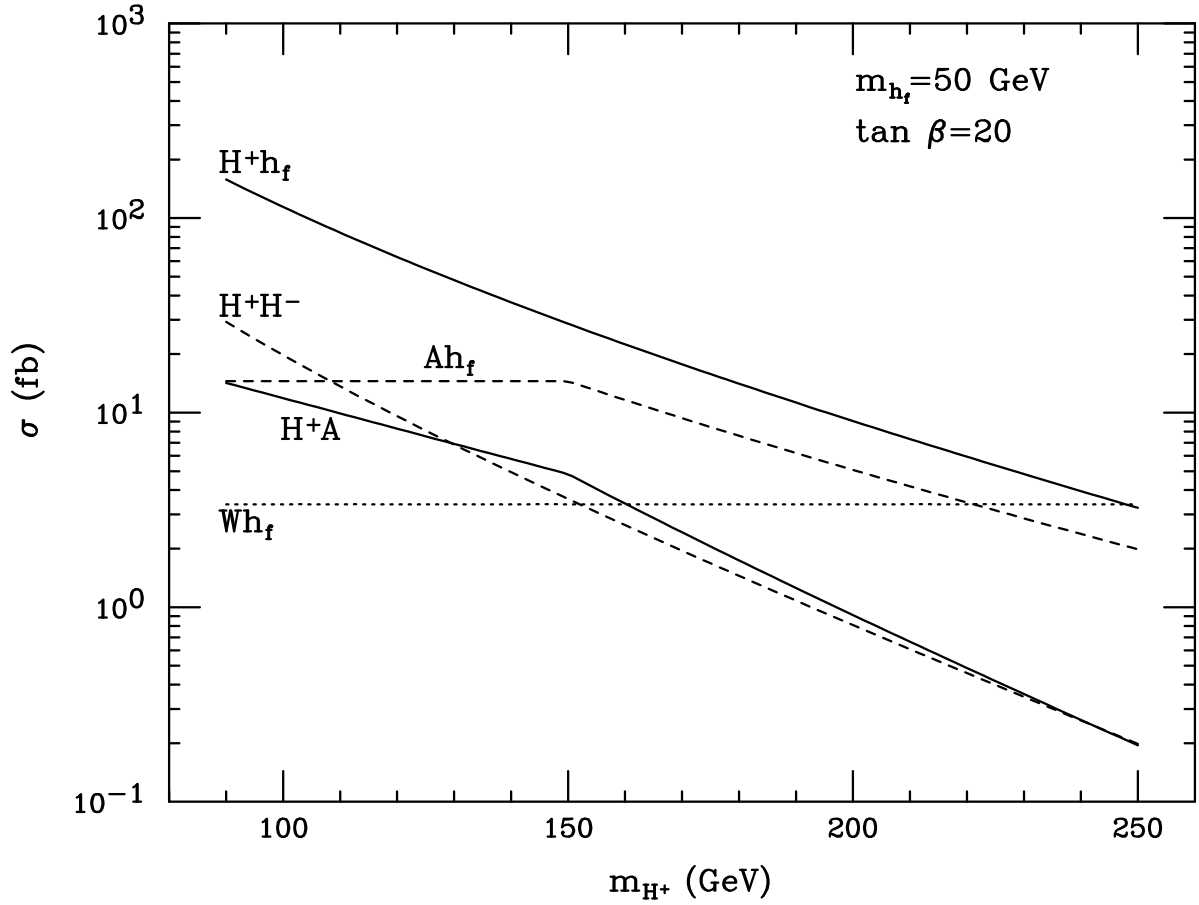


Figure 2: *Production cross section of five different modes leading to a fermiophobic Higgs boson as a function of the charged Higgs mass, for a fixed value of $\tan \beta$ and the fermiophobic Higgs mass (for the value of m_A , see the text).*

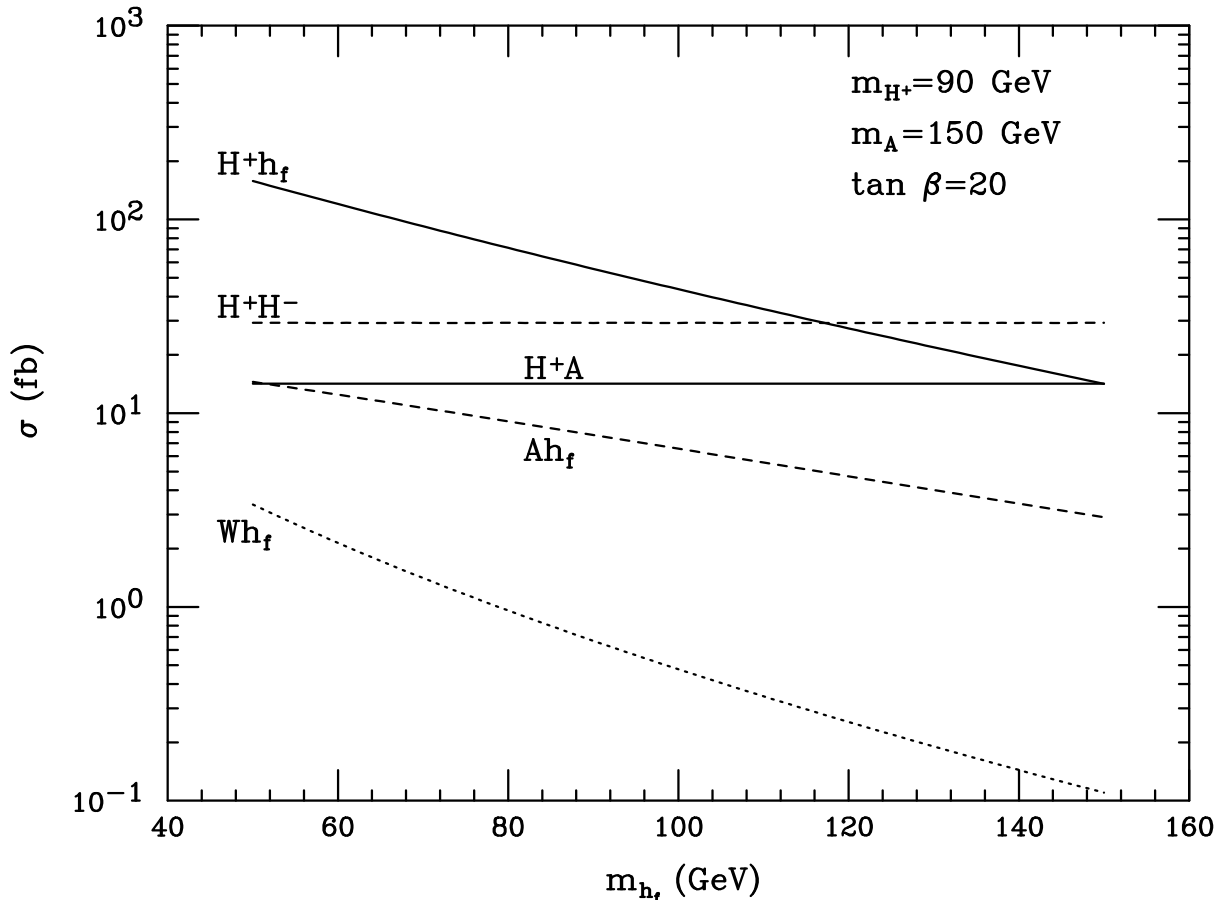


Figure 3: Production cross-section of five different modes leading to a fermiophobic Higgs boson as a function of the fermiophobic Higgs mass, for fixed values of $\tan \beta$, the charged and the CP-odd Higgs masses.

LEP2 in the process $e^+e^- \rightarrow h_f Z$. In order to compare cross-sections that depend on m_{H^+} , like $\sigma(p\bar{p} \rightarrow H^+h_f)$, with cross-sections that depend on m_A , like $\sigma(p\bar{p} \rightarrow A^0h_f)$, we have taken $m_A = m_{H^+}$ provided $m_A > 150 \text{ GeV}$. Nevertheless, when $m_{H^+} < 150 \text{ GeV}$ we keep a constant value $m_A = 150 \text{ GeV}$, which is required to satisfy the LEP constraint $m_{h_f} + m_A \geq 200 \text{ GeV}$. This is the explanation for the discontinuity in the slope of two of the cross-sections in Fig. 2. From the figure one can see that the traditional mechanism $p\bar{p} \rightarrow W^\pm h_f$ is severely suppressed ($\sigma \approx 3 \text{ fb}$ and independent of m_{H^+} and m_A), and there will not be enough events for its observation with the expected Run IIa integrated luminosity of 2 fb^{-1} .

As in the previous case, the process with the highest cross-section is $p\bar{p} \rightarrow H^\pm h_f$. Due to phase space, this cross-section decreases with the charged Higgs mass from $\sigma \approx 160 \text{ fb}$ for $m_{H^+} = 90 \text{ GeV}$ to $\sigma \approx 3 \text{ fb}$ for $m_{H^+} = 250 \text{ GeV}$. Only at these relatively high values of m_{H^\pm} does this cross-section become comparable with $\sigma(p\bar{p} \rightarrow W^\pm h_f)$. A similar behaviour, although with a much smaller cross-section, is also found for the process

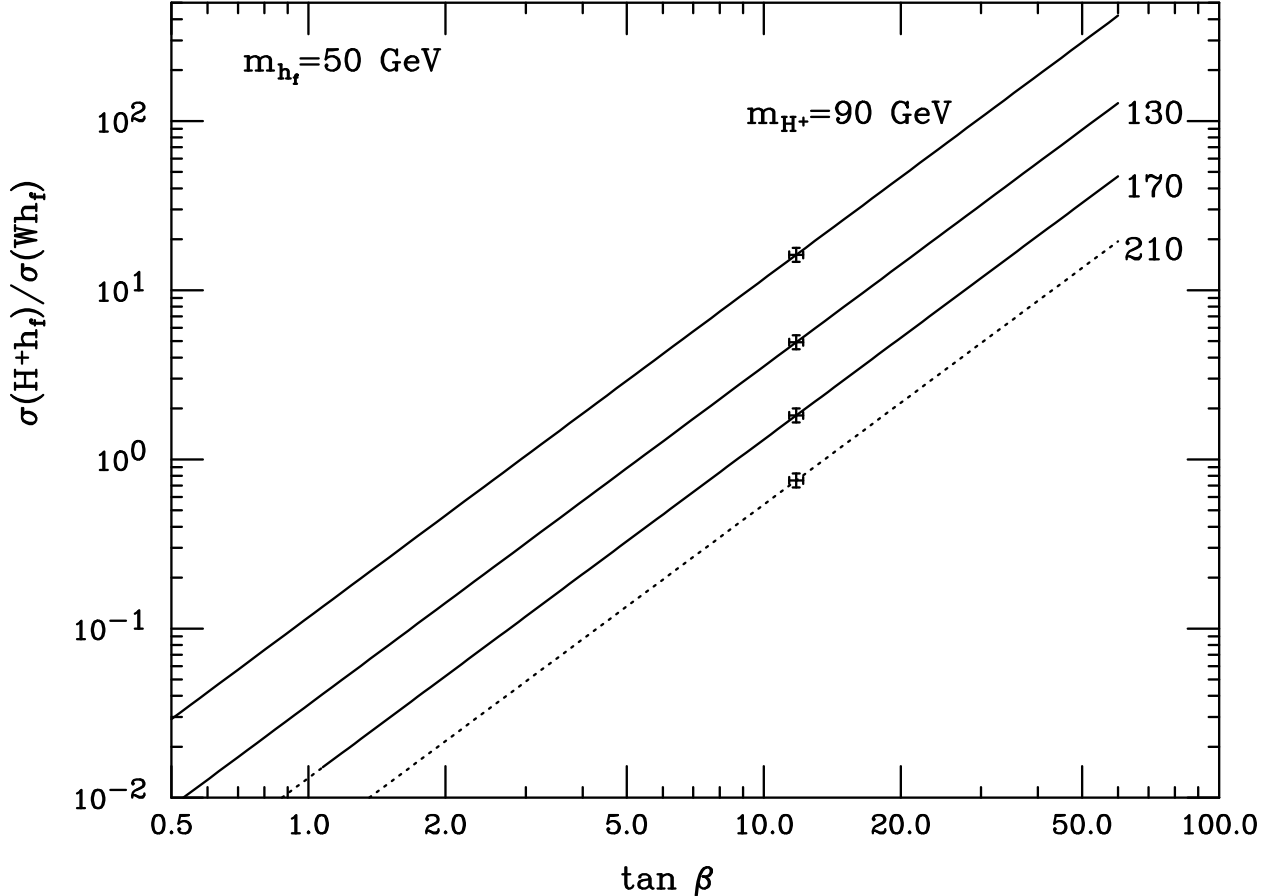


Figure 4: Ratio of $\sigma(p\bar{p} \rightarrow H^\pm h_f)$ and $\sigma(p\bar{p} \rightarrow W^\pm h_f)$ as a function of $\tan \beta$, for a fixed value of the fermiophobic Higgs mass and four different values of the charged Higgs mass.

$p\bar{p} \rightarrow H^+H^-$, with a cross-section decreasing from $\sigma \approx 30$ fb for $m_{H^\pm} = 90$ GeV to $\sigma \approx 0.2$ fb for $m_{H^\pm} = 250$ GeV. For most of the values of m_{H^\pm} and m_A shown in this graph, the subdominant mechanism is $p\bar{p} \rightarrow Ah_f$. Its cross-section remains constant at $\sigma \approx 15$ fb as long as $m_A = 150$ GeV. When m_A increases, the cross section decreases to $\sigma \approx 2$ fb for $m_A = 250$ GeV, and thus it is observable only for lower values of m_A . The last mechanism in this figure is $p\bar{p} \rightarrow H^+A^-$, and it is only observable for $m_{H^\pm} \lesssim 100$ GeV.

In Fig. 3 we plot the cross-sections as a function of m_{h_f} . For $m_{h_f} > 110$ GeV the decay $h_f \rightarrow VV^*$ becomes dominant. The figure shows the phase space suppression of increasing m_{h_f} . The large value of $\tan \beta = 20$ makes the traditional mechanism well suppressed and unobservable. The mechanism $p\bar{p} \rightarrow H^\pm h_f$ has a decreasing cross-section due to phase space, and it is the most favourable for $m_{h_f} \lesssim 120$. For larger values of the fermiophobic Higgs mass, $p\bar{p} \rightarrow H^+H^-$ becomes the largest cross-section (which is independent of m_{h_f}). Note that for $m_{h_f} > m_{H^\pm}$ the mechanism $p\bar{p} \rightarrow H^\pm h_f$ does not provide a V via the cascade decay of H^\pm , and thus only leads to a $\gamma\gamma$ signature. In addition, $p\bar{p} \rightarrow H^+H^-$ would not produce a h_f for $m_{h_f} > m_{H^\pm}$.

It is clear from the preceding figures that the production mechanism $p\bar{p} \rightarrow H^\pm h_f$ is usually the most favourable of the four alternatives we are analysing. Since all the mechanisms lead to the $\gamma\gamma V$ signature one could in principle add all the cross-sections together. In the remaining two figures we compare more closely $p\bar{p} \rightarrow H^\pm h_f$ and $p\bar{p} \rightarrow W^\pm h_f$.

In Fig. 4 we plot the ratio of $\sigma(p\bar{p} \rightarrow H^\pm h_f)$ and $\sigma(p\bar{p} \rightarrow W^\pm h_f)$ as a function of $\tan\beta$. We take the fermiophobic Higgs mass $m_{h_f} = 50$ GeV, and display four curves corresponding to different charged Higgs masses. As in Fig. 1, it is clear that the conventional production mechanism is convenient for low values of $\tan\beta$ and $p\bar{p} \rightarrow H^\pm h_f$ dominates for larger values of this parameter. The boundary lies somewhere between $\tan\beta = 3 \rightarrow 13$ with the larger values obtained for large charged Higgs masses. The cross on each curve marks the threshold of observability (which we take as 10 fb) for $\sigma(p\bar{p} \rightarrow W^\pm h_f)$, and corresponds to $\tan\beta \approx 12$. To the left of the crosses $\sigma(p\bar{p} \rightarrow W^\pm h_f) > 10$ fb, and to the right $\sigma(p\bar{p} \rightarrow W^\pm h_f) < 10$ fb. The solid lines correspond to $\sigma(p\bar{p} \rightarrow H^\pm h_f) \geq 10$ fb and dotted lines to $\sigma(p\bar{p} \rightarrow H^\pm h_f) \leq 10$ fb. As observed in Fig. 1, $\sigma(p\bar{p} \rightarrow H^\pm h_f)$ grows fast with $\tan\beta$, until it saturates at around $\tan\beta \approx 5$. This saturation value is $\sigma(p\bar{p} \rightarrow H^\pm h_f) = 158, 48, 18,$ and 7 fb for $m_{H^\pm} = 90, 130, 170,$ and 210 GeV respectively (the last one being unobservable).

Fig. 5 is the same as Fig. 4 but with $m_{h_f} = 100$ GeV. Here the conventional mechanism is unobservable for $\tan\beta \gtrsim 4$. The saturation values are $\sigma(p\bar{p} \rightarrow H^\pm h_f) = 44, 18, 8,$ and 4 fb for the same values of the charged Higgs mass. The new mechanism overcomes the conventional one in a larger region of parameter space since the ratio of cross-sections is larger than one for $\tan\beta \gtrsim 2 \rightarrow 7$, depending on the charged Higgs mass.

Given the sizeable cross-sections for $p\bar{p} \rightarrow H^\pm h_f$ this process (with h_f replaced by h^0) might have a wider application, e.g. in the search for H^\pm of any (non-SUSY) 2HDM. In particular this process is maximized in the parameter space of a light h^0 with suppressed couplings to vector bosons (i.e. small $\sin(\beta - \alpha)$).

5 Conclusions

We proposed new production mechanisms for light fermiophobic Higgs bosons (h_f) with suppressed couplings to vector bosons (V) at the Fermilab Tevatron. Importantly the new mechanisms offer sizeable cross-sections when the conventional process ($qq' \rightarrow W^\pm h_f$) is suppressed, and provide distinctive signatures with up to 4 photons. We showed that $qq' \rightarrow H^\pm h_f$ is particularly promising with cross-sections as large as 150 fb if both h_f and H^\pm are light (< 100 GeV). We suggested that the mechanism $qq' \rightarrow H^\pm h_f$ might also have a wider application in the search for a light h^0 and H^\pm of any general (non-SUSY) 2HDM.

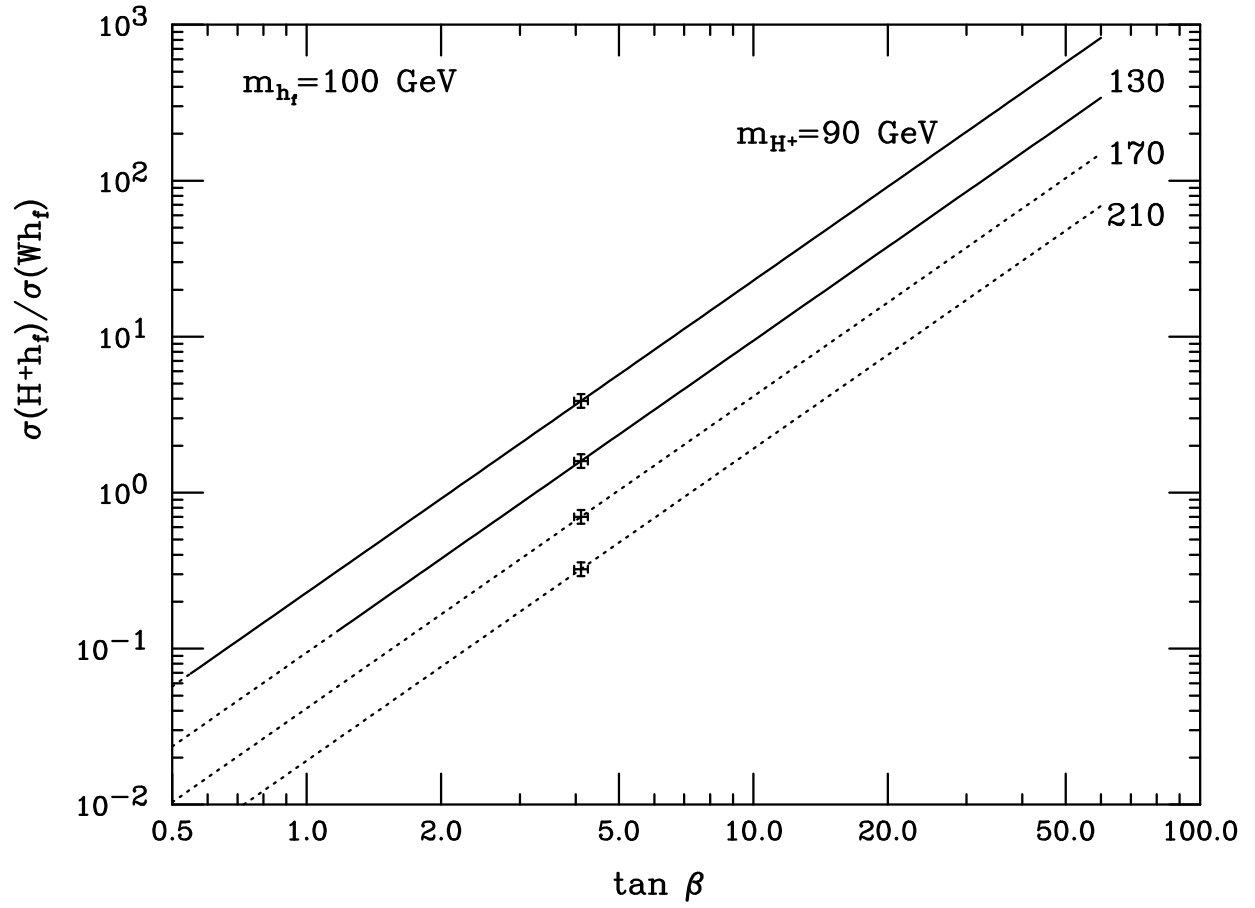


Figure 5: Ratio of $\sigma(p\bar{p} \rightarrow H^\pm h_f)$ and $\sigma(p\bar{p} \rightarrow W^\pm h_f)$ as a function of $\tan \beta$, for a fixed value of the fermiophobic Higgs mass and four different values of the charged Higgs mass.

Acknowledgements

A.G.A. expresses his gratitude to La Universidad Católica de Chile where part of this work was carried out. M.A.D. is thankful to Korea Institute for Advanced Study for their kind hospitality. Part of this work was financed by CONICYT grant No. 1010974.

References

- [1] J. F. Gunion, H. E. Haber, G. L. Kane and S. Dawson, “The Higgs Hunter’s Guide,” (Reading, MA: Addison-Wesley)
- [2] S. L. Glashow and S. Weinberg, *Phys. Rev. D* **15**, 1958 (1977).
- [3] V. D. Barger, J. L. Hewett and R. J. Phillips, *Phys. Rev. D* **41**, 3421 (1990).
- [4] A. G. Akeroyd, *Phys. Lett. B* **377**, 95 (1996); A. G. Akeroyd, *J. Phys. G* **24**, 1983 (1998)
- [5] G. Abbiendi *et al.* [OPAL Collaboration], *Eur. Phys. J. C* **18**, 425 (2001) A. Heister *et al.* [ALEPH Collaboration], *Phys. Lett. B* **544**, 25 (2002)
- [6] T. J. Weiler, *Proceedings of the 8th Vanderbilt Int. Conf. on High Energy Physics, Nashville, TN, Oct 8-10, 1987*; Edited by J. Brau and R. Panvini (World Scientific, Singapore, 1988), p219
- [7] H. E. Haber, G. L. Kane and T. Sterling, *Nucl. Phys. B* **161**, 493 (1979).
- [8] V. D. Barger, N. G. Deshpande, J. L. Hewett and T. G. Rizzo, arXiv:hep-ph/9211234. In Argonne 1993, Physics at current accelerators and supercolliders* 437-442.
- [9] H. Pois, T. J. Weiler and T. C. Yuan, *Phys. Rev. D* **47**, 3886 (1993)
- [10] A. Stange, W. J. Marciano and S. Willenbrock, *Phys. Rev. D* **49**, 1354 (1994)
- [11] M. A. Diaz and T. J. Weiler, arXiv:hep-ph/9401259.
- [12] A. G. Akeroyd, *Phys. Lett. B* **368**, 89 (1996)
- [13] A. Barroso, L. Brucher and R. Santos, *Phys. Rev. D* **60**, 035005 (1999)
- [14] L. Brucher and R. Santos, *Eur. Phys. J. C* **12**, 87 (2000); R. Santos, S. M. Oliveira and A. Barroso, arXiv:hep-ph/0112202.
- [15] G. Abbiendi *et al.* [OPAL Collaboration], *Phys. Lett. B* **544**, 44 (2002)
- [16] P. Abreu *et al.* [DELPHI Collaboration], *Phys. Lett. B* **507**, 89 (2001)
- [17] A. Heister *et al.* [ALEPH Collaboration], *Phys. Lett. B* **544**, 16 (2002).

- [18] P. Achard *et al.* [L3 Collaboration], Phys. Lett. B **534**, 28 (2002)
- [19] J. Mans, Nucl. Phys. Proc. Suppl. **109**, 130 (2002); A. Rosca [the LEP Collaborations], arXiv:hep-ex/0212038.
- [20] B. Abbott *et al.* [D0 Collaboration], Phys. Rev. Lett. **82**, 2244 (1999)
- [21] T. Affolder *et al.* [CDF Collaboration], Phys. Rev. D **64**, 092002 (2001)
- [22] H. Georgi and M. Machacek, Nucl. Phys. B **262**, 463 (1985). M. S. Chanowitz and M. Golden, Phys. Lett. B **165**, 105 (1985); J. F. Gunion, R. Vega and J. Wudka, Phys. Rev. D **42**, 1673 (1990); K. Cheung and D. K. Ghosh, JHEP **0211**, 048 (2002)
- [23] A. G. Akeroyd, Phys. Lett. B **442**, 335 (1998)
- [24] T. Han, A. S. Turcot and R. J. Zhang, Phys. Rev. D **59**, 093001 (1999)
- [25] S. Mrenna and J. Wells, Phys. Rev. D **63**, 015006 (2001)
- [26] G. Landsberg and K. T. Matchev, Phys. Rev. D **62**, 035004 (2000)
- [27] B. A. Dobrescu, G. Landsberg and K. T. Matchev, Phys. Rev. D **63**, 075003 (2001)
- [28] F. Larios, G. Tavares-Velasco and C. P. Yuan, Phys. Rev. D **64**, 055004 (2001); F. Larios, G. Tavares-Velasco and C. P. Yuan, Phys. Rev. D **66**, 075006 (2002)
- [29] A. G. Akeroyd, Nucl. Phys. B **544**, 557 (1999)
- [30] A. Djouadi, W. Kilian, M. Muhlleitner and P. M. Zerwas, Eur. Phys. J. C **10**, 45 (1999)
- [31] S. Kanemura and C. P. Yuan, Phys. Lett. B **530**, 188 (2002)
- [32] E. Eichten, I. Hinchliffe, K. D. Lane and C. Quigg, Rev. Mod. Phys. **56**, 579 (1984) [Addendum-ibid. **58**, 1065 (1986)].
- [33] S. Dawson, S. Dittmaier and M. Spira, Phys. Rev. D **58**, 115012 (1998)
- [34] A. D. Martin, R. G. Roberts, W. J. Stirling and R. S. Thorne, Eur. Phys. J. C **23**, 73 (2002)